Journal of Hazardous Materials 186 (2011) 667–674

Contents lists available at ScienceDirect

Journal of Hazardous Materials

journal homepage: www.elsevier.com/locate/jhazmat

Importance of carbon surface chemistry in development of iron–carbon composite adsorbents for arsenate removal

Eleni Deliyanni [b], Teresa J. Bandosz [a,*]

[a] Department of Chemistry, The City College of New York and The Graduate School of the City University of New York, Marshak Science Building, 138th Street and Convent Ave., New York, NY 10031, USA
[b] Department of Chemistry, Aristotle University of Thessaloniki 54124 Thessaloniki, Greece

ARTICLE INFO

Article history:
Received 2 June 2010
Received in revised form 25 October 2010
Accepted 12 November 2010
Available online 20 November 2010

Keywords:
Activated carbon
Surface chemistry
Impregnation
Arsenate adsorption

ABSTRACT

Micro/mesoporous activated carbon was oxidized and used either as received or after modification as a support for the deposition of iron oxyhydroxide. The prepared samples were applied as adsorbents of arsenate from water phase. The initial materials and those after adsorption were characterized using adsorption of nitrogen, – potentiometric titration, FTIR, EDX, XRD, AAS, and thermal analysis. The results obtained suggest that oxidation of the carbon support increases significantly the amount of iron oxyhydroxide species deposited on the surface and thus decreases their dispersions and the efficiency of arsenate immobilization in the carbon pore system. Iron hydroxyoxides react with arsenate forming salts. Moreover, a meso/microporous carbon surface contributes to changes in the toxicity of arsenic via reduction of As(V) to As(III). This is visible in the increased degree of carbon oxidation.

© 2010 Elsevier B.V. All rights reserved.

1. Introduction

A major water-born environmental problem is arsenic contamination of drinking water. Skin cancer, liver, lung, kidney, and bladder cancers as well as conjunctivitis, melanosis, hyperkeratosis, and in severe cases gangrene in the limbs and malignant neoplasm have been linked to arsenic toxicity [1].

Arsenic can exist in several forms in the environment. Both organic and inorganic compounds of arsenic are reported in natural waters. While latter ones dominate, the amount of organic arsenic in drinking water sources is insignificant. Arsenate (As(V)) and arsenite (As(III)) [2], are the arsenicals of concern in drinking water sources [3]. As(V) species are found in oxidizing environment, while As(III) are present in anoxic and reducing environments [4,5]. In ground water, the major species, As(V), exists as monovalent $H_2AsO_4^-$ and divalent $HAsO_4^{2-}$ anions resulting from the dissociation of arsenic acids (H_3AsO_4); while, As(III) species exists as uncharged arsenious acid (H_3AsO_3) [6,7].

Although background arsenic concentrations in natural water are low [8], elevated arsenic concentrations are common in groundwater. This is due to arsenic-bearing rocks which under favorable pH conditions mobilize the arsenic [9]. Human activities that could increase arsenic concentrations in groundwaters and surface waters include oil and coal burning power plants, waste incineration, cement works, disinfectants, household waste disposal, glassware production, electronics industries, ore production and processing, metal treatment, galvanizing, ammunition factories, dyes and colors, wood preservatives, pesticides, pyrotechnics, drying agents for cotton, oil and solvent recycling and pharmaceutical works [10,11]. Several countries such as Bangladesh, China, India, Argentina, Mexico, Peru, Hungary, Taiwan, Greece, Canada, United States, Japan, Poland, Serbia, Montenegro and Chile are affected by arsenic problems [12–19].

A variety of treatment techniques has been developed for the arsenic remediation from drinking water. Co-precipitation [20], sorption [21], ion flotation [22], foam flotation precipitation [20], bioremediation [22], solvent extraction [23], ion exchange [23], oxidation–reduction [24], and electrolysis and cementation [25], have been proposed to address the problem. Adsorption technology is the most common approach [26]. It is considered as an effective method, with a high removal efficiency and without harmful byproducts. A recent review on the arsenic removal by Mohan and Pittman gives a comprehensive idea about the different adsorptive processes investigated for the arsenic remediation [27].

The most widely studied media used as adsorbents include iron hydroxide and oxide (such as amorphous hydrous ferric oxide, ferrihydrite and goethite) [28–31], activated alumina [32,33], silica [34] and phyllosilicates [34], cellulose sponge [35], sand [36], zeolite [37] and activated carbon [38–40]. Recent research has focused on enhancing the effectiveness of sorbents by tailoring their specific properties in order to increase their affinity for contaminants. Mod-

* Corresponding author. Tel.: +1 212 650 6017; fax: +1 212 650 6107.
E-mail addresses: tbandosz@ccny.cuny.edu, tbandosz@sci.ccny.cuny.edu (T.J. Bandosz).

0304-3894/$ – see front matter © 2010 Elsevier B.V. All rights reserved.
doi:10.1016/j.jhazmat.2010.11.055

ified sorbents like iron oxide coated polymeric materials, iron oxide coated sand, lanthanum-impregnated silica gel, zirconia impregnated activated carbon, polyaniline modified granular activated carbon, iron-containing granular activated carbon, etc. have been used in the arsenic removal [41–44]. The combination of activated carbon and iron loading would take advantage of the strength of these two materials. It was shown that iron preloaded on the activated carbon surface offers high affinity for arsenate and arsenite ions [40,45–49]. The capacities reported for adsorption from a low concentration (less than 200 mg/L^{-1}) on the virgin carbon are in the range of few mg of As/g of adsorbents [27,40,42–50]. Iron oxide on the surface of carbon increases adsorption but still very seldom it is higher than 10 mg As/g of carbon [27,51,52]. It was suggested that iron species contribute to immobilization of arsenic via formation of complexes involving a ligand exchange with –OH and acid–base behavior [52], or via formation of metals arsenate [27]. These processes are pH dependent. The content of metal less than 6% was found as the most beneficial [40]. Besides iron, also other metals impregnated on carbon such as copper [51] or even those present in ash [50] were found as enhancing the arsenic removal efficiency.

Based on the results of the previous studies, which revealed that iron oxyhydroxide nanocrystals have a high affinity toward inorganic arsenic species and are very selective in the sorption process [53], the objective of this work is to further analyze the effect of the iron oxyhydroxide deposited in the pore system of carbon on the arsenate removal. To investigate the role of the carbons surface chemistry and structural heterogeneity in deposition of iron species and in adsorption or arsenate, the carbon surface was oxidized. The results are analyzed in terms of the effects of surface features on the capacity of carbon to adsorb arsenate.

2. Experimental

2.1. Materials

Wood based activated carbon BAX-1500 manufactured by Mead Westvaco was used in this study. The initial sample is designated as B. One sample of the carbon was oxidized with 70% HNO_3 for 4 h. The oxidation process, which usually results in the introduction of oxygen functional groups, was conducted by adding 100 mL of 70% nitric acid to 10 g of the BAX-1500 sample placed in a glass beaker with a magnetic stirrer. The mixture was stirred for 4 h. To remove an excess of acid and the soluble products of surface oxidation the carbon was extensively washed in a Soxhlet apparatus to constant pH. The oxidized sample was designated as BO.

The iron modified samples were prepared using a suspension of activated carbon or oxidized activated carbon in aqueous solutions of iron(III) nitrate (0.506 M with respect to Fe^{3+}) in a three-necked round-bottom flask, placed in a thermostat at 298 K. The precipitating agent (ammonium carbonate, 0.23 g/dm^3) was added dropwise, using a dosimetric pump (Metrohm 645 Multi-Dosimat) at a constant flow rate (0.15×10^{-4} dm^3/s) until the final pH of the hydrolysis process, measured with a Crison MicropH 2002 instrument, was adjusted to 8. Vigorous mechanical stirring at 620 rpm was applied in order to achieve good mixing of the reactants and to prevent a possible agglomeration of the gel. After the addition of the precipitating agent, the stirring was continued for at least 15 min. The product obtained was decanted in a dialysis tubing cellulose membrane (Sigma Co.), and placed in a bath of distilled water. Upon standing, the anions of the suspension were removed by osmosis through the membrane. The water of the bath was replaced until no more anions were detectable in it. The resulting cake, on the membrane surface, was freeze-dried by a bench-scale instrument (Christ Alpha 1–4), until the temperature of the frozen gel reached the ambient temperature. The samples after the iron modification are referred to as BFe and BOFe following the notification used for the initial samples. The sample exposed to arsenate have letter E added to their names.

2.2. Methods

2.2.1. Adsorption of arsenate from solution

Arsenate stock solution (1000 mg L^{-1}) was prepared by dissolving reagent-grade 4.1653 g $Na_2HAsO_4{\cdot}7H_2O$ of 99.8% purity (AnalaR) into 1 L of distilled water. Working solutions were prepared fresh daily for each batch test.

The batch experiments for the arsenate removal from dilute aqueous solutions were carried out at an ambient temperature, using deionised water and suitable conical flasks (10 mL sample volume), agitated with a reciprocal shaker (160 rpm) for 24 h. This contact time allows the equilibrium to be reached, as determined in the separate experiments. The pH was kept at about 5.5 to ensure the presence of the same arsenic species. At this pH range arsenate exists mainly as $H_2AsO_4^-$ and $HAsO_4^{2-}$ [53,54]. The final pH in all cases was measured and found to change of about ±0.5. It is assumed that these changes do not affect the speciation of arsenate ions in the solutions.

The adsorption isotherms which represent the amount of arsenic adsorbed per gram of carbon were obtained by varying the arsenate concentrations under a fixed dose of an adsorbent. For the sorption experiments, the sorbent concentrations of 0.05 g L^{-1} were applied while the arsenate concentrations were from 10 to 150 ppm As. The residual arsenic, i.e. that remaining in the solution after the application of a solid/liquid separation of suspended solids by a 0.45 m membrane filtration, was chemically analyzed. The molybdenum blue method was followed, using a double-beam UV–visible spectrophotometer (Hitachi Model U-2000) according to the appropriate standard method. This method is based on the development of the molybdate–arsenate complex [55,56]. As(3+) is oxidized with $KBrO_3$ to As(5+) which reacts with ammonium molybdate forming arsenomolybdate salt [57,58]. This salt, at about 90 °C, in the presence of hydrazine sulfate, is reduced to a blue molybdate complex, which is called molybdenum blue. The absorbance was measured at 800 nm.

Samples not analyzed on the same day of adsorption experiment, were acidified to about pH 1 with concentrated HCl and stored in acid-washed high-density polyethylene containers. All samples were analyzed within three days of collection.

The quantity of As sorbed was expressed as adsorption isotherms using the Langmuir–Freiundich equation [60]:

$$\vartheta_t = \frac{q_e}{q_o} = \frac{KC^n}{1 + (KC)^n} \quad (1)$$

where q_e is the adsorbed amount of the solute per unit gram of an adsorbent, q_o is its maximum adsorption per unit weight of the adsorbent, K is the Langmuir-type constant defined by the Van't Hoff equation, and the exponential term n represents the heterogeneity of the site energies. The fitting range was for equilibrium concentration from 0 to 100 mg As/kg.

2.2.2. Potentiometric titration

Potentiometric titration (PT) measurements were performed with a DMS Titrino 716 automatic titrator (Metrohm, Brinkmann Instruments, Westbury, NY, USA). The instrument was set in the equilibrium mode when the pH was collected. Approximately 0.1000-g samples were placed in a container thermostatted at 25 °C with 50 mL of 0.01 M $NaNO_3$ and equilibrated overnight. To eliminate any interference by dissolved CO_2, the suspension was continuously saturated with N_2. The carbon suspension was stirred throughout the measurement. Each sample was titrated

with 0.1 MNaOH titrant using 0.001-mL increments. Experiments were carried out from the initial pH of the suspension.

The surface properties were evaluated assuming that the population of sites can be described by a continuous pK_a distribution, $f(pK_a)$. The experimental data can be transformed into a proton binding isotherm, Q, representing the total amount of protonated sites, which is related to the pK_a distribution by the following integral equation

$$Q(\mathrm{pH}) = \int_{-\infty}^{\infty} q(\mathrm{pH}, pK_a) f(pK_a)\, dpK_a \quad (2)$$

The solution of this equation is obtained using the numerical procedure, which applies regularization combined with non-negativity constraints. Based on the spectrum of acidity constants and the history of the samples, the detailed surface chemistry was evaluated [61].

2.2.3. pH

The pH of a carbon sample provides information about the acidity or the basicity of the surface. A sample of 0.4 g of dry carbon powder was added to 20 mL of water, and the suspension was stirred overnight to reach equilibrium. Then the pH of the solution was measured.

2.2.4. Surface area and pore size distribution measurements

Nitrogen isotherms were measured using an ASAP 2010 (Micromeritics) at 77 K. Before the experiment the samples were heated at 393 K and then outgassed at this temperature under a vacuum of 10^{-4} Torr to constant pressure. The isotherms were used to calculate the specific surface area (S_{BET}), that was calculated from the isotherm data using the Brunauer, Emmet and Teller (BET) model, volume of pores smaller than 10 Å, $V < 10$ Å, volume of micropores, V_{mic}, volume of mesopores, V_{mes}, and total pore volume, V_t, calculated using density functional theory (DFT).

2.2.5. Thermal analysis

Thermal analysis was carried out using a TA Instrument thermal analyzer (SDT). The instrument settings were a heating rate of 10 K/min and a nitrogen atmosphere with a 100 mL/min flow rate. For each measurement about 25 mg of a ground carbon sample was used.

2.2.6. FTIR

FTIR spectroscopy was carried out using a Nicolet Magna-IR 830 spectrometer using the attenuated total reflectance method (ATR). The spectrum was generated and collected 16 times and corrected for the background noise. The experiments were done on the powdered samples, without KBr addition.

2.2.7. SEM/EDAX

Scanning electron microscopy (SEM) images were performed at Zeiss Supra 55 VP. The accelerating voltage was 15.00 kV. Scanning was performed in situ on a sample powder. EDAX analysis was done at magnification 10 K and led to the maps of elements.

2.2.8. XRD

The crystal structure of the samples was examined by X-ray diffraction. Powder XRD patterns were recorded with a Siemens D500 X-ray diffractometer with autodivergent slit and graphite monochromator using Cu K_a radiation, with a scanning speed of $2^\circ\ min^{-1}$.

2.2.9. AAS

To test the iron loading on carbon, 0.2 g of carbon was ashed at 600 °C and then digested with 25 mL of concentrated hydrochloric acid. The digestion solutions were analyzed for iron by a Perkin Elmer AAnalyst 400 Atomic Adsorption Spectophotometer.

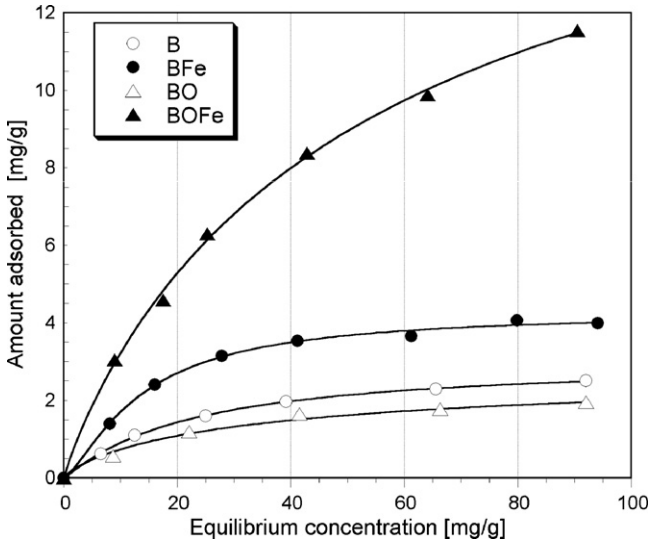

Fig. 1. Arsenic adsorption isotherms. Solid lines represent the fitting to Langmuir–Freundich equation.

3. Results and discussion

The measured isotherms of arsenate adsorption on the carbons studied are collected in Fig. 1 along with the fit to Langmuir–Freundlich isotherms. The fitting parameters are reported in Table 1. Although oxidation decreases the adsorption capacity of the carbon likely as a result of ash removal [56,57], an introduction of iron species to the oxidized samples has a well marked positive effect on the adsorption of arsenate. The performance of the BOFe is about six times better than that of the initial carbon. The adsorption capacities are in the order of those reported in the literature for modified carbons [27,40,50–52,60]. The K values should be related to the energy of adsorption and apparently they are much higher on the unoxidized samples than those on oxidized. This suggests differences in the mechanism of adsorption. Introduction of iron has opposite effects on the K values for both B and BO. The n values are related to the surface heterogeneity, which refers to both, diversity in pore sizes and in the chemistry of the adsorption sites (Table 1). The values higher than 1 indicate a more diverse surface from the point of view of the adsorption sites and it certainly is a case for B and BFe in which K values were the highest. Chuang and co-workers suggested that $n > 1$ indicates the favorable adsorption at a low concentration [52].

To clearly understand positive effects of modifications applied to the as received BAX-1500 carbon, the porosity and surface chemistry of the initial and exposed to arsenate adsorbents have to be analyzed in details. Parameters of the porous structure calculated from nitrogen adsorption isotherms are collected in Table 2. As seen, oxidation severely affected the porosity of carbons. Pore volumes and surface areas decreased about 50%. Modification with iron further decreases the porosity of the oxidized sample and

Table 1
Fitting parameters to Langmuir–Freundlich equation and the goodness of the fit.

Sample	q_o (mg As/g)	K (L/mg)	n	R^2
B	3.03	0.045	1.07	0.9995
BO	2.85	0.028	0.82	0.9887
BFe	4.28	0.074	1.38	0.9973
BOFe	18.90	0.018	0.92	0.9987

Table 2
Parameters of the pore structure calculated from nitrogen adsorption isotherms.

Sample	S_{BET} (m^2/g)	$V<10$ Å (cm^3/g)	V_{mic} (cm^3/g)	V_{mes} (cm^3/g)	V_t (cm^3/g)
B	2143	0.12	0.69	0.80	1.49
BE	1218	0.15	0.24	0.51	0.75
BFe	1765	0.11	0.51	0.66	1.17
BFeE	1528	0.09	0.43	0.58	1.01
BO	1175	0.15	0.28	0.48	0.76
BOE	1068	0.18	0.14	0.48	0.62
BOFe	765	0.12	0.12	0.33	0.45
BOFeE	697	0.12	0.08	0.31	0.39

the surface areas of the initial and oxidized carbons are reduced of about 18% and 35%. This is the result of the deposition of 5.3% or iron in the case of BFe sample, and 31% in the case of BOFe. Interestingly, adsorption of arsenate affects the surface of the B sample to greatest extent (of 43%) suggesting a blockage of porosity by the adsorbate or by surface reaction products. On the other hand, the surface of the BOFe sample after adsorption of a large quantity of arsenate decreased only about 10%. This indicates the difference in the mechanisms of adsorption related to the variety of surface chemistry and thus to the heterogeneity of the adsorption sites.

Details on the porosity changes are seen on pore size distributions collected in Fig. 2. While for both samples without iron exposed to arsenate the significant contributions of the pore volume in mesopores are not accessible for nitrogen molecules, for BOFeE only pores larger than 30 Å seem to be slightly affected. An opposite effect is seen upon the modification with iron where for BOFe the volume in all pores decreases compared to the BO. Only a slight effect in pores larger then 10 Å is seen for the unoxidized sample, BFe. These differences are certainly linked to the differences in the content of iron.

Apparently these differences in the iron distribution are expected to be related to the chemistries of the carbon support. Proton binding curves measured by titration with a base to avoid reactions of iron with an acid are collected in Fig. 3. As expected, oxidation causes visible changes in acidity of the carbon support. The BO sample shows only a proton release process. Modification with iron makes the surface more basic on the average in the case of oxidized sample while only a slight change is noticed in the pH of the initial sample (Table 3). In the case of both carbons the total number of acidic groups detected in the experimental window decreased, which suggests either their involvement in the iron deposition or it is just related to the blocking of the porosity by the deposited iron species. In fact, the later scenario is expected to have a much

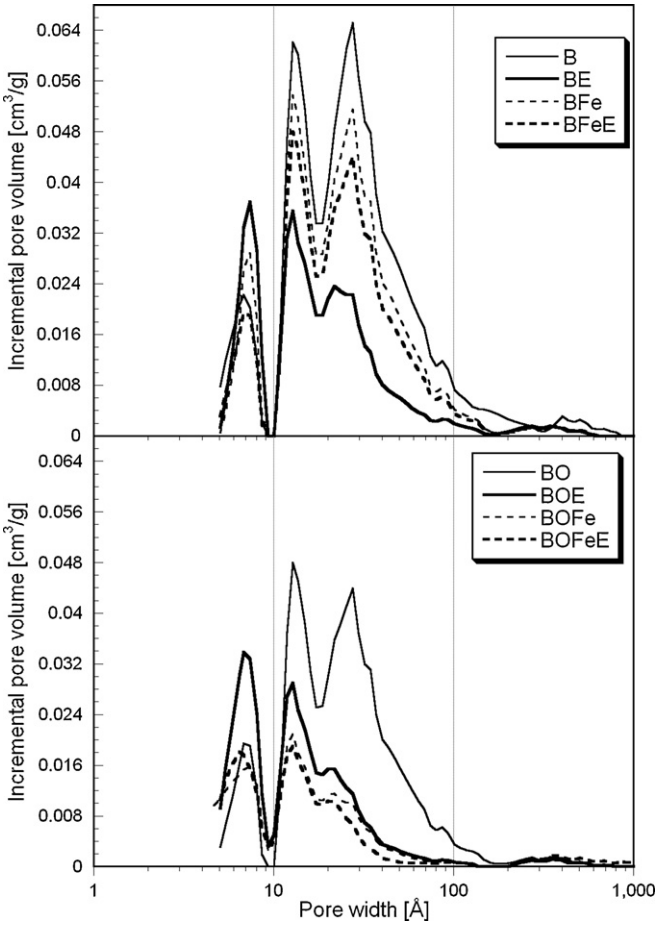

Fig. 2. Pore size distributions for the samples studied.

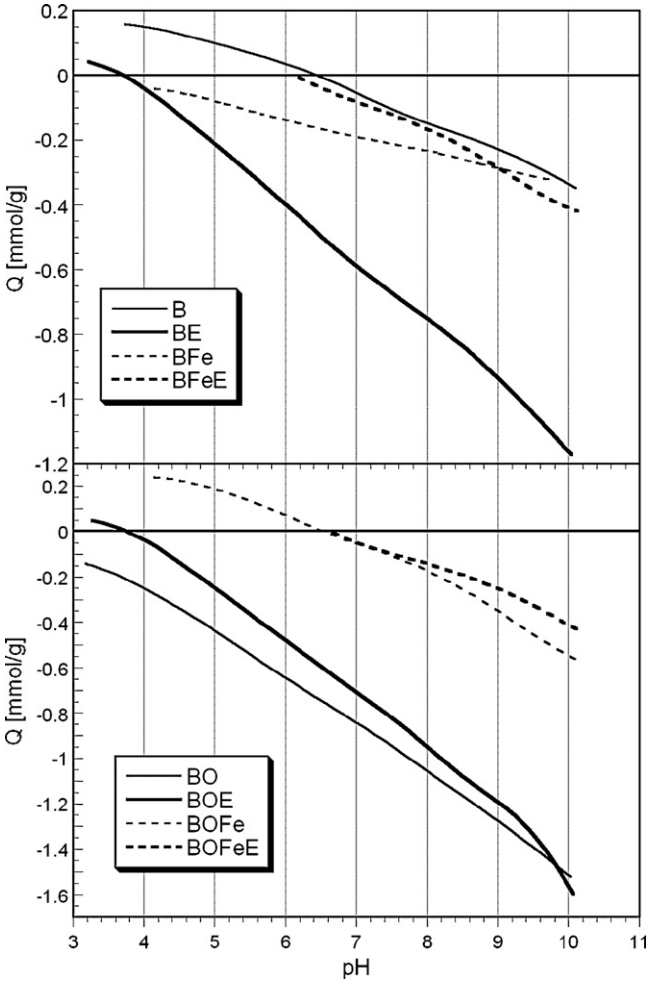

Fig. 3. Proton binding curves for the samples studied.

more pronounced effect in the case of BOFe carbon whose surface decreased to much larger extent than that for BFe, as discussed above. After the exposure to arsenate the number of acidic groups of the samples without iron increased noticeably. While it resulted in an increase in the average pH for the oxidized samples, the B sample became more acidic. This increase in acidity of the carbon without iron can be linked either to the physical adsorption of the arsenic acid or the oxidation of the surface by As(V). Although this hypothesis opposes the finding of Pattanayak and co-workers who suggested that carbon oxygen groups contribute to oxidation of As(III) [50] we will support our assumption by the experimental results obtained. Following this, As(III) (As_2O_3) would be formed along with the new oxygen containing groups attached to the carbon matrix. While for BO–E these new groups seem to be phenols with $pK_a > 9$, in the case of B the species with the whole spectrum of pK_a are present on the carbon surface after the exposure to arsenate. This hypothesis is consistent with the ability of the carbon surface to act as a reductant [62]. When that surface is already oxidized the number of sites being able to accept oxygen is drastically reduced, which is reflected in our experimental results. The samples with iron exposed to arsenate show a visible decrease in the acidity, which suggests reactions of iron oxide/hydroxides with arsenate anions and formation of salts. This was indicated by Lorenzen and co-workers [51] who suggested formation of $Fe(AsO_4)_2$, $FeAsO_4 \times Fe(OH)_3$ and $FeAsO_4 \times H_2O$. Mohan and Pittman proposed the following reaction [27]:

$$FeOOH + 3H_2AsO_4^- + 3H^+ \rightarrow Fe(H_2AsO_4)_3 + 2H_2O \quad (I)$$

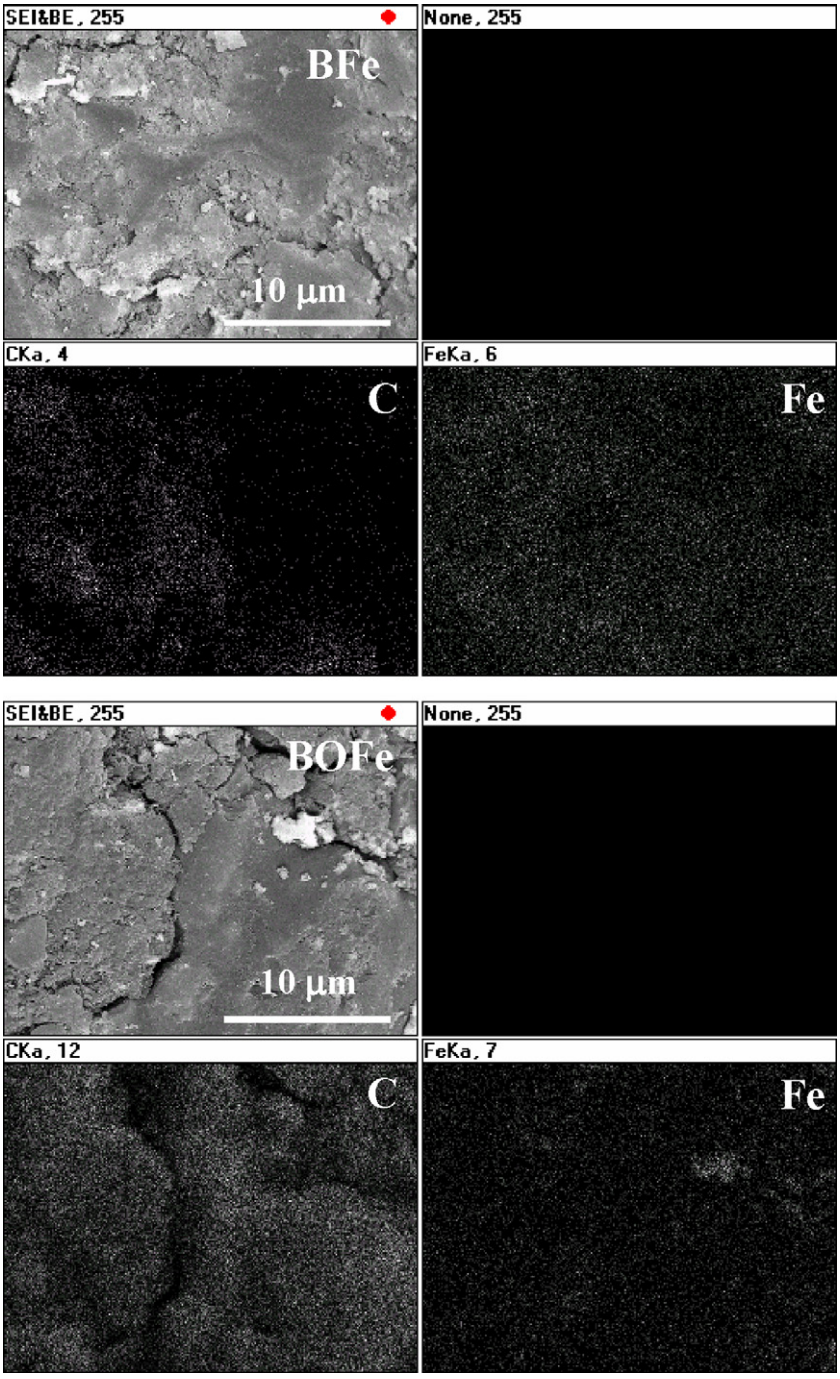

Fig. 4. EDX maps.

Table 3
Iron content, the numbers of all acidic, weakly acidic ($pK_a < 8$) and strongly acidic groups ($pK_a > 8$) calculated form potentiometic titration data (in mmol/g).

Sample	Fe_{AAS} (wt.%)	Fe_{XPS} (wt.%)	pH	All	$pK_a > 8$	$pK_a < 8$
B	0	0	5.84	0.838	0.525	0.323
BE	ND	ND	4.28	1.436	0.562	0.874
BFe	5.3	4.9	5.52	0.345	0.176	0.169
BFeE	ND	ND	6.23	0.401	0.288	0.113
BO	0	0	3.36	1.933	1.045	0.888
BOE	ND	ND	4.13	2.205	1.344	0.861
BOFe	31.0	29.2	4.84	1.250	0.733	0.517
BOFeE	ND	ND	6.31	0.734	0.352	0.382

The modification of carbons with iron used in our experimental approach intended to introduce iron in the form of iron oxyhydroxide. In Table 3 we report the iron content determined using AAS and XPS. Although discrepancies exist and they can be linked to the specificities of the methods, consistently BOFe has much more iron than BFe. This high content of iron oxide can be responsible for the significant change in the porosity of this carbon. As mentioned above, the iron oxide deposited in larger pores can block the smaller ones, or it acts as a phase, which causes an apparent "dissolution" of the porous carbon phase. Nevertheless, apparently the iron content, not the surface area, governs the capacity of our carbons for As removal. The high dispersion of iron on the surface of carbons is seen on EDAX maps presented in Fig. 4. For BOFe the larger clusters of iron species are detected than for BFe owing to the differences in chemical compositions. The ratio of adsorbed arsenic atoms to iron deposited on the surface is 0.06 for BFe and 0.045 BOFe. This result shows the higher efficiency of iron involvement on the surface of unoxidzied carbon, which can be explained by its higher dispersion of the active species on the surface, owing to its smaller iron content. In the case of BOFe the majority of iron centers, especially those existing in the clusters, are likely not accessible for As.

Some effects of the exposure of carbon to iron species and then to arsenate should be seen on DTG curves obtained in nitrogen where the weight loss is associated to the removal/decomposition of species present on the carbons surface (Fig. 5). The above hypothesis about the oxidation of the carbon surface when exposed to arsenate is supported by broad peaks on DTG curves between 200 and 800 °C. They resemble those seen on the DTG for BO curves and are the result of the decomposition of oxygen containing groups [62]. When the B carbon is modified with iron the weight loss is expected to be related to the gradual dehydratation/dehydroxylation of iron oxyhydroxides. These oxyhydroxides get finally reduced in two steps to metallic iron between 750 and 900 °C [57,63]. When arsenate is adsorbed on the BFe sample the reduction pattern on iron oxide changes. The peaks shift to lower temperature and an additional weight loss is seen as a shoulder at $T > 800$ °C. This might represent the reduction of iron arsenate formed as a result of reactive adsorption [27]. More heterogeneity in the reduction of iron species is also seen on the DTG curves for BOFeE where the second peak of iron reduction is spread out over 100 °C. Interestingly, after arsenate adsorption a new peak appears at about 800–900 °C, which might be linked to the decomposition of oxygen groups formed as a result of oxidation of this carbon surface. An increase in the number of phenols was indicated from the analysis of the potentiometric titration data and they should decompose at this temperature range.

To further evaluate the chemistry XRD analysis was carried out but unfortunately, owing to the amorphous phases of iron oxide and small amounts of arsenate adsorbed no diffraction peaks were measured. The differences are seen on FTIR spectra collected in Fig. 6. The band at about 1600 cm^{-1} is the combination of C=C stretching vibration of the aromatic ring structures (1590 cm^{-1}) and conjugated systems such as diketone, ketoester, quinone

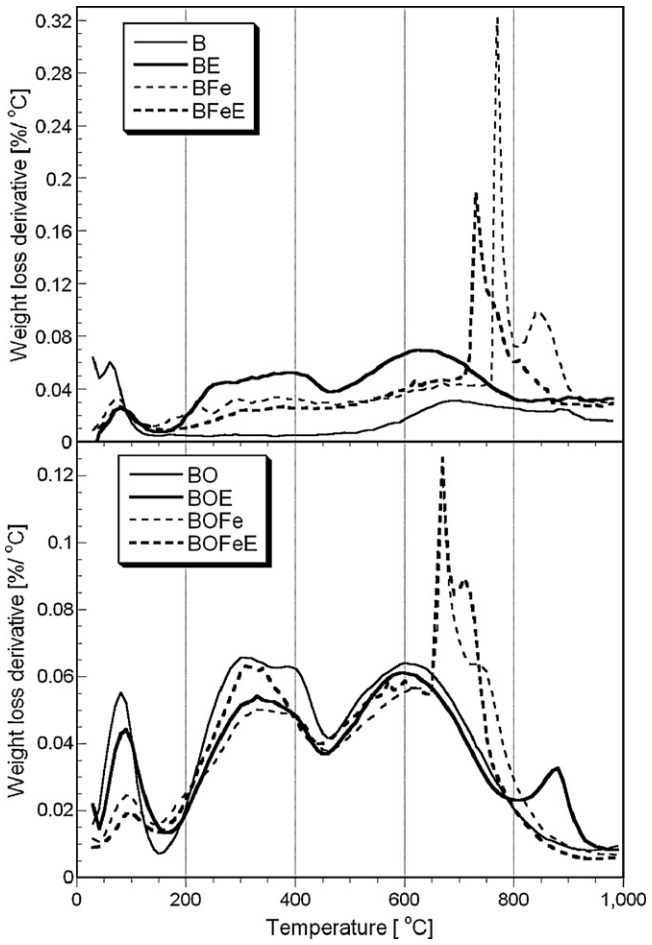

Fig. 5. Comparison of the DTG curves in nitrogen for the initial and exhausted samples.

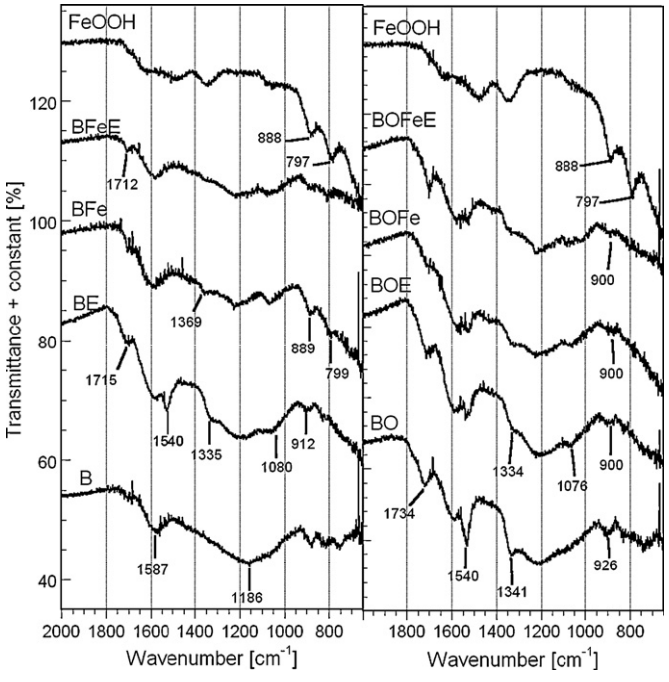

Fig. 6. FTIR spectra for B and BO series of samples.

(1550–1680 cm^{-1}). A broad band from about 1300 cm^{-1} to about 1000 cm^{-1} is assigned to C–O–C lactone structures, stretching C–O vibrations of phenol structures and ethers and bending O–H modes of phenol structures and a band at about 950 cm^{-1} represents epoxy groups. After the adsorption of arsenate on the B sample, an increase in the intensity of those bands is observed, as well as new bands at 1714 cm^{-1} corresponding to the carboxyl C=O stretching of non-aromatic carboxylic acid and at 1540, 1335, 1080 cm^{-1} corresponding to the stretching of carboxylate and to phenols [64]. For this sample a band at 912 cm^{-1} attributed to the presence As(III) is seen [65]. An increase in the intensity of the band at 950 cm^{-1} supports the presented above data suggesting oxidation of this carbon surface as a result of the exposure to arsenate. The intensity of the bands representing oxygen groups is obviously much higher for the oxidized sample (BO) than for the B sample. On the spectra for FeOOH the peaks at about 888 cm^{-1} and 797 cm^{-1} are characteristic for the goethite phase [66], while the peaks at the region 1300–1650 cm^{-1} are assigned to carbonate species adsorbed on the iron oxyhydroxide [67]. The peaks due to goethite are much more visible for BFe than for BOFe, owing to the high content of the iron phase in the latter sample. After the adsorption of the arsenates, the intensity of these peaks is smaller suggesting that iron oxyhydroxide has reacted with arsenate. The bands at about 800 cm^{-1} (not so visible) are attributed to the presence of As(V) [59].

4. Conclusions

The results presented in this paper suggest that oxidation of the carbon support increases significantly the amount of iron oxyhydroxide species deposited on the surface and thus decreases their dispersions and the efficiency of arsenate immobilization in the carbon pore system. These species react with arsenate forming salts. Moreover, meso/microporous carbon surface contributes to changes in the toxicity of arsenic via reduction of As(V) to As(III). This is visible in the increased degree of carbon oxidation.

Acknowledgement

The help of Dr. Mykola Seredych is appreciated.

References

[1] C.K. Jain, I. Ali, Arsenic: occurrence, toxicity and speciation techniques, Water Res. 34 (2000) 4304–4312.
[2] P.L. Smedley, H.B. Nicolli, D.M.J. Macdonald, A.J. Barros, J.O. Tullio, Hydrogeochemistry of arsenic and other inorganic constituents in groundwaters from La Pampa, Argentina, Appl. Geochem. 17 (2002) 259–284.
[3] X.C. Le, Arsenic speciation in the environment and humans, in: J. William, T. Frankenburger (Eds.), Environmental Chemistry of Arsenic, Marcel Dekker Inc., New York, 2002.
[4] H.L. Lien, R.T. Wilkin, High level arsenite removal from ground water by zero-valent iron, Chemosphere 59 (2005) 377–386.
[5] S. Kundu, A.K. Gupta, Sorption kinetics of As(V) with iron oxide coated cement – a new adsorbent and its application in the removal of arsenic from real-life ground water sample, J. Environ. Sci. Health A 40 (2005) 2227–2246.
[6] I. Bodek, W.J. Lyman, W.F. Reehl, D.H. Rosenblatt (Eds.), Environmental Inorganic Chemistry, Pergamon Press, New York, 1988.
[7] J. Hlavay, K. Polyak, Determination of surface properties of iron hydroxide coated alumina adsorbent prepared from drinking water, J. Colloid Interface Sci. 284 (2005) 71–77.
[8] L.S. Clesceri, A.E. Greenberg, R.R. Trussell, M.A. Franson, Standard Methods for the Examination of Water and Wastewater, 19th ed., American Public Health Association, Washington, DC, 1992.
[9] K.A. Francesconi, D. Kuehnelt, in: W.T. Frankenberger Jr. (Ed.), Arsenic Compounds in the Environment, Environmental Chemistry of Arsenic, Marcel Dekker, New York, 2002, p. 56.
[10] J. Matschullat, Arsenic in the geosphere, Sci. Total Environ. 249 (2000) 297–312.
[11] M. Berg, H.C. Tran, T.C. Nguyen, H.V. Pham, R. Schertenleib, W. Giger, Arsenic contamination of groundwater and drinking water in Vietnam: a human health threat, Environ. Sci. Technol. 35 (2001) 2621–2626.
[12] A.H. Smith, E.O. Lingas, M. Rahman, Contamination of drinking water by arsenic in Bangladesh: a public health emergency, Bull. WHO 78 (2000) 1093–1103.
[13] L. Zhang, C.J. Chen, Geographic distribution and exposure of drinking water with high concentration of arsenic in China, J. Hyg. Res. 26 (1997) 310–313.
[14] M.M. Rahman, U.K. Chowdhury, S.C. Mukherjee, B.K. Mandal, K. Paul, D. Lodh, Chronic arsenic toxicity in West Bengal, India – a review and commentary, Toxicology 39 (2001) 683–700.
[15] T. Agusa, K. Takagi, R. Kubota, Y. Anan, H. Iwata, S. Tanabe, Specific accumulation of arsenic compounds in green turtles (Chelonia mydas) and hawksbill turtles (Eretmochelys imbricata) from Ishigaki Island, Japan, Environ. Pollut. 153 (2008) 127–136.
[16] M. Walker, R.L. Seiler, M. Meinert, Effectiveness of household reverse-osmosis systems in a Western U.S. region with high arsenic in groundwater, Sci. Total Environ. 389 (2008) 245–252.
[17] S.J. McLaren, N.D. Kim, Evidence for a seasonal fluctuation of arsenic in New Zealand's longest river and the effect of treatment on concentrations in drinking water, Environ. Pollut. 90 (1995) 67–73.
[18] J.C. Ng, J. Wang, A. Shraim, A global health problem caused by arsenic from natural sources, Chemosphere 52 (2003) 1353–1359.
[19] United Nations Educational Scientific and Cultural Organization (UNESCO), Proceedings of the Press Conference on Launching an Anti-Arsenic Water Filter, 10th October 2005, UNESCO Press, 7 Place de Fontenoy, 75352 Paris 07 SP, France, 2005.
[20] P. Mondal, C.B. Majumder, B. Mohanty, Laboratory based approaches for arsenic remediation from contaminated water: recent developments, J. Hazard. Mater. 137 (2006) 464–479.
[21] S. Atkinson, Filtration technology verified to remove arsenic from drinking water, Membr. Technol. 3 (2006) 8–9.
[22] I.A. Katsoyiannis, A.I. Zouboulis, Application of biological processes for the removal of arsenic from groundwaters, Water Res. 38 (2004) 17–26.
[23] J. Kim, M.M. Benjamin, Modeling a novel ion exchange process for arsenic and nitrate removal, Water Res. 38 (2004) 2053–2062.
[24] K.V. Hege, M. Verhaege, W. Verstraete, Electro-oxidative abatement of low-salinity reverse osmosis membrane concentrates, Water Res. 38 (2004) 1550–1558.
[25] N. Balasubramanian, K. Madhavan, Arsenic removal from industrial effluent through electrocoagulation, Chem. Eng. Technol. 24 (2001) 519–521.
[26] World Health Organization (WHO), Guidelines for Drinking-Water Quality, vol. 1, second ed., WHO, Geneva, 1993.
[27] D. Mohan, C.U. Pittman Jr., Arsenic removal from water/wastewater using adsorbents – a critical review, J. Hazard. Mater. 142 (2007) 1–53.
[28] S. Fendorf, M.J. Eick, P. Grossl, D.L. Sparks, Arsenate and chromate retention mechanism on goethite. 1. Surface structure, Environ. Sci. Technol. 31 (1) (1997) 315–320.
[29] W. Driehaus, M. Jekel, U. Hiildebrandt, Granular ferric hydroxide – a new adsorbent for the removal of arsenic from natural water, J. Water SRT Aqua 47 (1998) 30–35.
[30] C.A.J. Appelo, V.D. Weiden, C. Tournassat, L. Charlet, Surface complexation of ferrous iron and carbonate on ferrihydrite and the mobilization of arsenic, Environ. Sci. Technol. 36 (2002) 3096–3103.
[31] K.P. Raven, A. Jain, R.H. Loeppert, Arsenite and arsenate adsorption on ferrihydrite: kinetics, equilibrium, and adsorption envelope, Environ. Sci. Technol. 32 (3) (1998) 344–349.
[32] T.S. Singh, K.K. Pant, Equilibrium, kinetic and thermodynamic studies for adsorption of As(III) on activated alumina, Sep. Purif. Technol. 36 (2) (2004) 139–147.
[33] S. Kuriakose, T.S. Singh, K.K. Pant, Adsorption of As(III) from aqueous solution onto iron oxide impregnated activated alumina, Water Qual. Res. J. 39 (3) (2004) 258–266.
[34] Y. Xu, L. Axe, Synthesis and characterization of iron oxide-coated silica and its effect on metal adsorption, J. Colloid Interface Sci. 282 (2005) 11–19.
[35] J.A. Munoz, A. Gonzalo, M. Valiente, Arsenic adsorption by Fe(III)-loaded open-celled cellulose sponge. thermodynamic and selectively aspects, Environ. Sci. Technol. 36 (14) (2002) 3405–3411.
[36] S.L. Lo, T.H. Jeng, L.H. Chin, Characteristics and adsorption properties of an iron-coated sand, Water Sci. Technol. 35 (1997) 63–70.
[37] M.S. Onyango, Y. Kojima, H. Matsuda, A. Ochieng, Adsorption kinetics of arsenic removal from groundwater by iron-modified zeolite, J. Chem. Eng. Jpn. 36 (12) (2003) 1516–1522.
[38] C.P. Huang, P.L.K. Fu, Treatment of arsenic (V)-containing water by the activated carbon process, J. Water Pollut. Control. Fed. 56 (3) (1984) 233–241.
[39] R.L. Vaughan Jr., B.E. Reed, Modeling As(V) removal by a iron oxide impregnated activated carbon using the surface complexation approach, Water Res. 39 (6) (2005) 1005–1014.
[40] Z. Gu, J. Fang, B. Deng, Preparation and evaluation of GAC-based iron-containing adsorbents for arsenic removal, Environ. Sci. Technol. 39 (10) (2005) 3833–3843.
[41] L. Yang, S. Wu, J.P. Chen, Modification of activated carbon by polyaniline for enhanced adsorption of aqueous arsenate, Ind. Eng. Chem. Res. 46 (2007) 2133–2140.
[42] V.K. Gupta, V.K. Saini, N. Jain, Adsorption of As(III) from aqueous solutions by iron oxide-coated sand, J. Colloid Interface Sci. 288 (2005) 55–60.
[43] B. Daus, R. Wennrich, H. Weiss, Sorption materials for arsenic removal from water: a comparative study, Water Res. 38 (2004) 2948–2954.
[44] K.D. Hristovski, P.K. Westerhoff, T. Möller, P. Sylvester, Effect of synthesis conditions on nano-iron (hydr)oxide impregnated granulated activated carbon, Chem. Eng. J. 146 (2009) 237–243.

[45] P. Mondal, C.B. Majumder, B. Mohanty, Effects of adsorbent dose, its particle size and initial arsenic concentration on the removal of arsenic, iron and manganese from simulated ground water by Fe^{3+} impregnated activated carbon, J. Hazard. Mater. 150 (2008) 695–702.
[46] G. Muñiz, V. Fierro, A. Celzard, G. Furdin, G. Gonzales-Sánchez, M.L. Ballinas, Synthesis, characterization and performance in arsenic removal of iron-doped activated carbons prepared by impregnation with Fe(III) and Fe(II), J. Hazard. Mater. 165 (2009) 893–902.
[47] V. Fierro, G. Muñiz, G. Gonzales-Sánchez, M.L. Ballinas, A. Celzard, Arsenic removal by iron-doped activated carbon prepared by ferric chloride forced hydrolysis, J. Hazard. Mater. 168 (2009) 430–437.
[48] H. Zhu, Y. Jia, X. Wu, H. Wang, Removal of arsenic from water by supported nano zero-valent iron on activated carbon, J. Hazard. Mater. 172 (2009) 1591–1596.
[49] W. Chen, R. Parette, J. Zou, F.S. Cannon, B.A. Dempsey, Arsenic removal by iron-modified activated carbon, Water Res. 41 (2007) 1851–1858.
[50] J. Pattanayak, K. Modal, S. Mathew, S.B. Lalvani, A parametric evaluation of the removal of As(V) and As(III) by carbon based adsorbents, Carbon 38 (2008) 589–596.
[51] L. Lorenzen, J.S.J. Deventer van, W.M. Landi, Factors affecting the mechanism of the adsorption of arsenic species on activated carbon, Mater. Eng. (1995) 557–569.
[52] C.L.D. Chuang, M. Fan, M. Xu, R.C. Brown, S. Sung, B. Saha, C.P. Hunag, Adsorption of arsenic (V) by activated carbon prepared from oat hulls, Chemosphere 61 (2005) 478–483.
[53] M.X. Loukidou, K.A. Matis, A.I. Zouboulis, M. Liakopoulou-Kyriakidou, Removal of As(V) from wastewaters by chemically modified fungal biomass, Water Res. 37 (2003) 4544–4552.
[54] Mineql+, Environmental Research Software, Hallowell, USA, 1994.
[55] E.B. Sandell, Colorimetric Determination of Traces of Metals, Interscience, New York, 1965.
[56] I.M. Kolthoff, P.J. Elving (Eds.), Treatise in Analytical Chemistry, Interscience, New York, 1962.
[57] A.S.T.M., Chemical Analysis of Metals and Metal Bearing Ores, Des. E87-58, Reappr. 1978, Part 12, U.S.A. (1982).
[58] J. Rodier, Analysis of Water, Wiley, New York, 1975.
[59] E.A. Deliyanni, D.N. Bakoyannakis, A.I. Zouboulis, K.A. Matis, Sorption of As(V) ions by akaganeite-type nanocrystals, Chemosphere 50 (2003) 155–163.
[60] A. Derylo-Marczewska, M. Jaroniec, D. Gelbin, A. Seidel, Heterogeneity effects in single-solute adsorption from dilute solutions on solids, Chem. Scr. 24 (1984) 239–246.
[61] J. Jagiello, T.J. Bandosz, J.A. Schwarz, Carbon surface characterization in terms of its acidity constant distribution, Carbon 32 (1994) 1026–1028.
[62] C.O. Ania, T.J. Bandosz, Metal-loaded polystyrene-based activated carbons as dibenzothiophene removal media via reactive adsorption, Carbon 44 (2006) 2404–2412.
[63] D. Hines, A. Bagreev, T.J. Bandosz, Surface properties of porous carbon obtained from polystyrene sulfonic acid-based organic salts, Langmuir 20 (2004) 3388–3397.
[64] S. Biniak, G. Szymańnski, J. Siedleweski, A. Swiatkowski, The characterization of activated carbons with oxygen and nitrogen surface groups, Carbon 35 (1997) 1799–1803.
[65] C. Petit, G.W. Peterson, J. Mahle, T.J. Bandosz, The effect of oxidation on the surface chemistry of sulfur-containing carbons and their arsine adsorption capacity, Carbon 48 (2010) 1779–1787.
[66] P.S.R. Prasad, K.S. Prasad, V.K. Chaitanya, E.V.S.S.K. Babu, B. Sreedhar, S. Ramana Murthy, In situ FTIR study on the dehydration of natural goethite, J. Asian Earth Sci. 27 (2006) 503–511.
[67] I. Carabante, M. Grahn, A. Holmgren, J. Kumpiene, J. Hedlund, Adsorption of As(V) on iron oxide nanoparticles films studied by in situ ATR-FTIR spectroscopy, Colloids Surf. A: Physicochem. Eng. Aspects 346 (2009) 106–113.